AiMT

Advances in Military Technology
Vol. 13, No. 2 (**2018**), pp. 237-248
ISSN 1802-2308, eISSN 2533-4123
DOI 10.3849/aimt.01243

Ballistics of Supercavitating Projectiles

D. Nguyen Thai[1], V. Horák[2*], D. Nguyen Van[1], D. Dao Van[1],
H. Nguyen Van[1] and L. Do Duc[2]

[1] *Department of Weapons, Le Quy Don Technical University, Hanoi, Vietnam*
[2] *Faculty of Military Technology, University of Defence in Brno, Czech Republic*

The manuscript was received on 27 March 2018 and was accepted after revision for publication on 10 September 2018.

Abstract:

The article is focused on the development of the underwater ballistic model of a supercavitating projectile fired from an underwater firearm. The supercavitating flows and their influences on the ballistic characteristics of the projectile are studied. The presented mathematical model is validated and experimentally verified for the supercavitating projectile of 5.7 mm in diameter fired from a smooth bore underwater rifle.

Keywords:

underwater projectile, supercavitation, cavity, underwater ballistics, supercavitating ammunition

1. Introduction

Underwater firearms are designed for underwater use and they are being utilized in armed forces of various nations. Their common feature is that they have smooth bores and fire supercavitating underwater projectiles instead of standard ammunition because the standard bullets do not work well underwater.

One of engineering challenges in designing underwater ammunition is that of developing a projectile, which can satisfy the requirements for the effective firing range and the firing accuracy.

The underwater ballistics is of high practical significance in designing the underwater projectiles. Based on the underwater ballistics solutions, we are able to define the ballistic characteristics of the supercavitating projectile, which plays a crucial role in underwater ammunition designing.

The moving of the underwater projectile in water is very different from when the projectile is shooting in air. A significant phenomenon taking place when the underwater projectile travels in water is a supercavitation, i.e. the appearance of vapour

* *Corresponding author: University of Defence in Brno, Kounicova 65, 662 10 Brno, Czech Republic. Phone: +420 973 44 26 16, E-mail: vladimir.horak@unob.cz*

bubbles and pockets inside water. This phenomenon strongly influences the stability of the projectile motion and the drag force against the projectile motion. The hydrodynamic scheme of supercavitation flow, when the projectile is placed fully inside a supercavity, is shown in Fig. 1 [1].

There are almost no available sources closely documenting the external ballistics of the underwater firearms when the supercavitation processes are taking place. Hence, in this paper, a novel mathematical underwater ballistic model is proposed by considering the influences of the supercavitating flows and the interaction of the projectile rear with the supercavity. The developed mathematical model has been validated and experimentally verified.

2. Mathematical Model

2.1. Features of Supercavitating Flows

When the underwater projectile exits the barrel muzzle, a supercavity (Fig. 1) around the projectile is formed. According to the supercavitating flow configuration, it can take various figures. Cavitation affects creating bubbles of steam and cavities large enough to encompass the projectile travelling through an initially homogeneous liquid medium. Changes in physical properties of fluid significantly reduce the skin friction drag on the projectile and enable the projectile to achieve very high speeds.

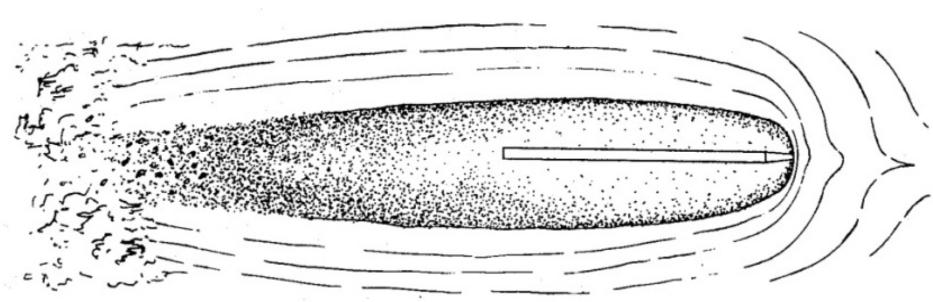

Fig. 1 Scheme of projectile supercavitating motion [1]

In general, the mechanism of supercavities formation can be explained by three phases as follows [2]:

- Phase I – cavitation inception: This phase is characterized by the creation of small vapour bubbles.
- Phase II – partial cavitation: In this phase, the cavitation is partially formed and the vapour bubbles grow unstably.
- Phase III – fully developed supercavitation: In this phase, the supercavity is fully developed and encompasses the projectile. The supercavity shape is close to the elliptical form.

The supercavitating flow starts when the underwater projectile head is moving out of the barrel muzzle. The supercavity is fully developed when the maximum length L_C and the maximum radius R_C are reached (Fig. 2).

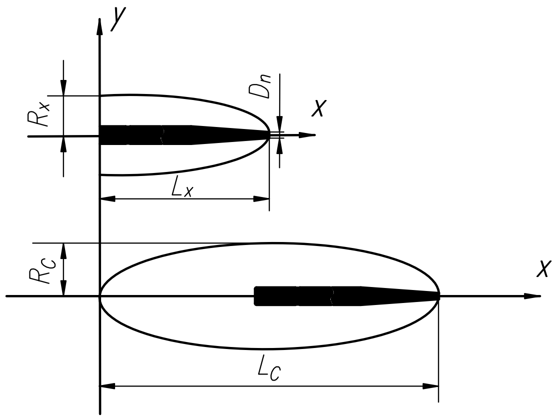

Fig. 2 Scheme of supercavity formation

If we assume the supercavity of elliptical shape [2], then its geometry is given by

$$\frac{x^2}{\left(\frac{L_c}{2}\right)^2} + \frac{y^2}{R_c^2} = 1\,, \tag{1}$$

where L_c and R_c account for the maximum length and maximum radius of the supercavity, respectively. For underwater projectiles with a disk nose, the values of L_C and R_c can be calculated by Eqs (2) and (3)

$$L_c = \frac{D_n}{\sigma}\sqrt{C_{x0}\left(1+\sigma\right)\ln\frac{1}{\sigma}}\,, \tag{2}$$

$$R_c = \frac{D_n}{2}\sqrt{\frac{C_{x0}\left(1+\sigma\right)}{\sigma}}\,, \tag{3}$$

where D_n denotes the underwater projectile disk nose diameter. The nose part of projectile is called cavitator. Further, C_{x0} is the cavitator drag coefficient for the cavitation number $\sigma = 0$. The cavitation number is the main scaling criterion of the supercavitation flows, which is defined as

$$\sigma = \frac{2\,\Delta p}{\rho v^2}\,, \tag{4}$$

where Δp is the pressure difference in the free stream and cavity, v is the fluid velocity, and ρ is the fluid density.

When values of cavitation number σ are small, from 0.012 to 0.057, for underwater projectiles with the disk cavitator it is established that $C_{x0} = 0.82$ [4].

2.2. Equations of Motion for Underwater Projectile

The system of equations modelling the underwater projectile motion is built on the basis of the following assumptions:

- The projectile is a homogeneous rigid body symmetric about the x-axis.
- The projectile is fired from the smooth bore barrel. Hence, the rotation about the projectile axis of symmetry can be neglected.

- No influences of other factors inside the cavity, such as water droplets, water vapour and powder gas.
- The projectile can rotate about its nose.
- Water is considered to be the viscous and incompressible fluid as the homogeneous and isotropic continuum.
- The mass of projectile is constant and its centre of mass position is not changing during the projectile motion.
- The projectile nose has the disk cavitator, which is perpendicular to the *x*-axis.
- The influence of gravity, buoyancy and surface tension forces on the projectile dynamics are neglected.

In order to describe the underwater projectile motion, the Descartes coordinate system has been established at the mass centre of the projectile O_1 as shown in Fig. 3, where:

- x_1-axis represents the horizontal axis of the projectile symmetry;
- x_0-axis corresponds to the velocity vector of projectile mass centre;
- y_1-axis and y_0-axis are perpendicular to both *x*-axes of the projectile in the vertical direction;
- O_1K is the line on the vertical plane of x_1-axis, where the velocity vector $\boldsymbol{v}$ is projected;
- α is the angle between the x_1-axis and O_1K;
- β is the angle between the x_0-axis and O_1K.

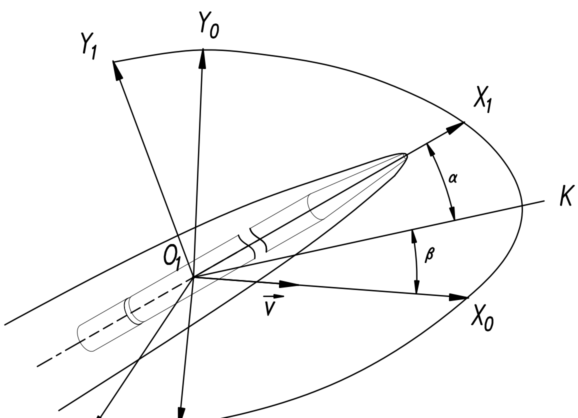

Fig. 3 Coordinate system at the projectile mass centre

In addition, we also use a coordinate system *O, x, y, z* that is related to the earth. Then, we can describe the projectile motion in the vertical plane as bellow:

$$m\left(\frac{dv_{x_1}}{dt} - \omega_y v_{y_1}\right) = F_{x_1},$$
$$m\left(\frac{dv_{y_1}}{dt} - \omega_z v_{x_1}\right) = F_{y_1}. \quad (5)$$

$$I_z \frac{d\omega_{z_1}}{dt} = M_{z_1}, \qquad \omega_z = \frac{d\psi}{dt}, \tag{6}$$

where:

- m is the mass of the projectile;
- v_{x_1} is the x_1-component of the projectile mass centre velocity vector;
- v_{y_1} is the y_1-component of the projectile mass centre velocity vector;
- $\omega_y, \omega_z, \omega_{z_1}$ are the angular velocities of the projectile about y-axis, z-axis and z_1-axis, respectively;
- ψ is the angle of yaw;
- F_{x_1}, F_{y_1} are x_1- and y_1-components of the resultant force acting on the projectile mass centre;
- M_{z_1} is the resultant torque acting on the projectile about the z_1-axis;
- I_z is the moment of inertia of the projectile about the z-axis.

The velocity of the projectile v can be calculated by

$$v = \sqrt{v_{x_1}^2 + v_{y_1}^2}, \tag{7}$$

$$v_{x_1} = v\cos\alpha\cos\beta, \qquad v_{y_1} = -v\sin\alpha\cos\beta. \tag{8}$$

From Eq. (8), we can express the angle α as a function of the projectile velocity components as

$$\alpha = -\arctan\frac{v_{y_1}}{v_{x_1}}. \tag{9}$$

Then, we can rewrite equations from (5) to (9) to the system of equations describing the motion of the projectile in the final form as bellow:

$$\begin{aligned} v\cos(\psi-\alpha)\frac{dv_{x_1}}{dx} &= \omega_z v_{y_1} + \frac{1}{m}F_{x_1}, \\ v\cos(\psi-\alpha)\frac{dy_1}{dx} &= -\omega_z v_{x_1} + \frac{1}{m}F_{y_1}, \\ v\cos(\psi-\alpha)\frac{d\psi}{dx} &= \omega_z, \\ \frac{dy}{dx} &= \tan(\psi-\alpha). \end{aligned} \tag{10}$$

The total time $t(x)$, in which the projectile has travelled a distance s from the origin of the coordinate system, is given by

$$t(x) = \int_0^x \frac{ds}{v\cos(\psi-\alpha)}. \tag{11}$$

2.3. Calculation of Forces Acting on Projectile

There are two main forces acting on the projectile moving underwater:

- The nose drag force F_n.
- The hydrodynamic force F_s acting on the tail of the projectile due to the projectile interaction with the supercavity.
- The gravity, buoyancy and surface tension forces are neglected.

The nose disk plane changes its position during the projectile motion underwater due to the interaction of the projectile with the supercavity [5]. Therefore, the coordinate system O_n, x_n, y_n, z_n for the nose of the projectile is established, as shown in Fig. 4.

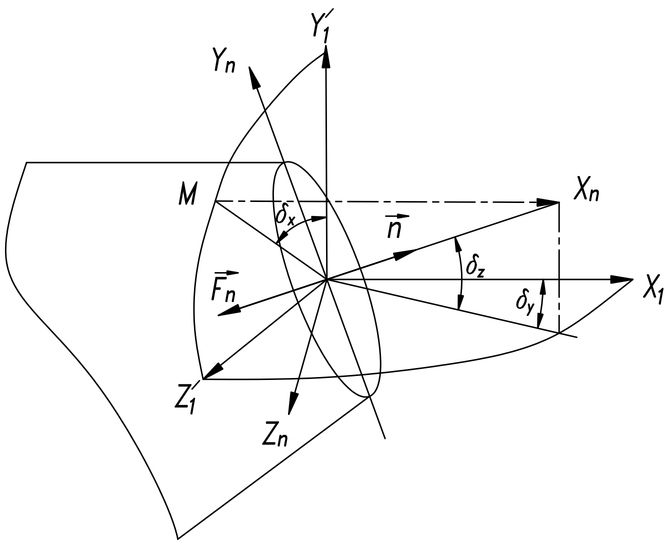

Fig. 4 Coordinate system of projectile nose

The nose drag force is given by

$$F_n = F_{x0} \cos \mu \,, \tag{12}$$

where μ is the angle between the water flow direction and the projectile x_n-axis.

The nose drag force F_{x0}, when the nose disk cavitator is perpendicular to the water flow direction, is given by the following formula

$$F_{x0} = C_{x0} \left(1+\sigma\right). \tag{13}$$

We can express the projection of vector F_n to each axis of O_n, x_n, y_n, z_n coordinate system as

$$\begin{aligned} F_{nx} &= -F_n \cos \delta_y \cos \delta_z, \\ F_{ny} &= -F_n \sin \delta_z, \\ F_{nz} &= F_n \sin \delta_y \cos \delta_z. \end{aligned} \tag{14}$$

In the vertical direction, the interactive hydrodynamic force F_s acting on the tail of projectile due to interaction with the cavity can be calculated by the Wagner's method [6-8] as

$$F_{sy} = \rho \pi R_s^2 v_0 \left[v_1 \frac{\bar{h}\left(2+\bar{h}\right)}{\left(1+\bar{h}\right)^2} + v_2 \frac{2\bar{h}}{1+\bar{h}} \right]. \tag{15}$$

Here, v_0 is the water mainstream velocity, v_2 is the relative velocity of the cavity related to the projectile and v_1 is the velocity of the tail of the projectile in the vertical plane.

The value of $\bar{h}$ appearing in Eq. (15) is given by formula

$$\bar{h} = \frac{h}{R_c - R_s}, \tag{16}$$

in which h is the height of the wetted part of the projectile tail. Values of R_c and R_s are radii of the supercavity and the projectile at the point of impact with the cavity.

The horizontal component of the interactive hydrodynamic force vector F_s is given by the friction force as

$$F_{sx} = \frac{\rho v^2}{2} A_w C_f \left(\mathrm{Re}_w\right). \tag{17}$$

The drag force coefficient C_f of the projectile is an experimental function of the Reynolds number of water flows

$$\mathrm{Re}_w = \frac{\rho l_w v}{\eta}, \tag{18}$$

where l_w and A_w are the length and the surface area of the wetted part of the projectile, η is the dynamic viscosity and ρ is the density of water.

3. Validation of the Model

The mathematical model described above is applied for the case of 5.7 mm underwater cartridge. The mass of the projectile is 0.026 kg and the projectile length is 115 mm. The view of the underwater cartridge is shown in Fig. 5 and the engineering drawing of the underwater projectile is given in Fig. 6.

The projectile is fired from the smooth ballistic barrel located underwater in the depth of 1 m. The muzzle velocity is 254 m·s $^{-1}$.

The mathematical model developed in this study was solved numerically in the MATLAB programming environment. Some results of solution are presented in graphs from Fig. 7 to Fig. 10.

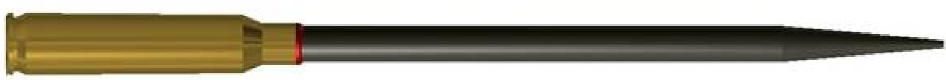

Fig. 5 View of 5.7 mm *underwater cartridge*

The calculated parameters of the fully developed supercavity are given in Fig. 7. The supercavity maximum length is L_c = 319.3 mm and the supercavity maximum radius is R_c = 8.3 mm.

The time variation of the nose drag force and the force acting at the tail of the projectile due to its interaction with the supercavity are shown in Fig. 8 and Fig. 9.

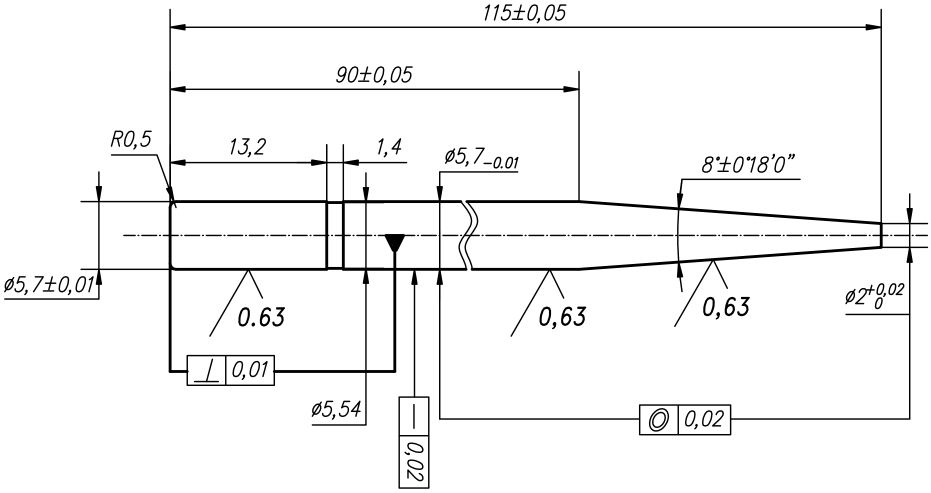

Fig. 6 Engineering drawing of the 5.7 mm *underwater projectile*

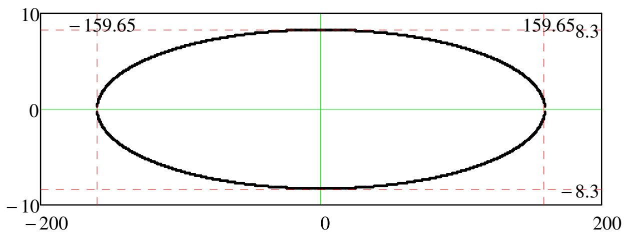

Fig. 7 Supercavity calculated parameters in [mm]

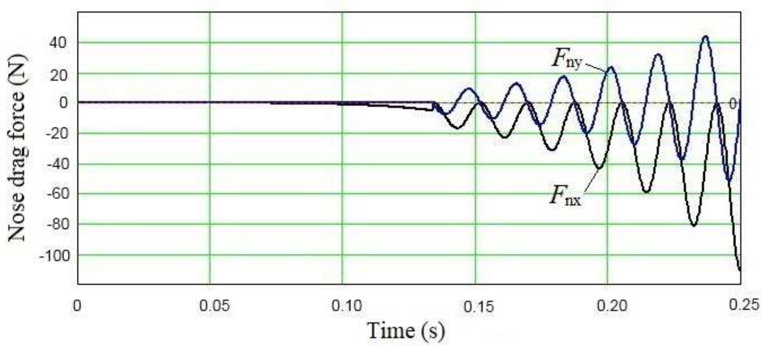

Fig. 8 Nose drag force vs. time in vertical F_{ny} *and in horizontal* F_{nx} *direction*

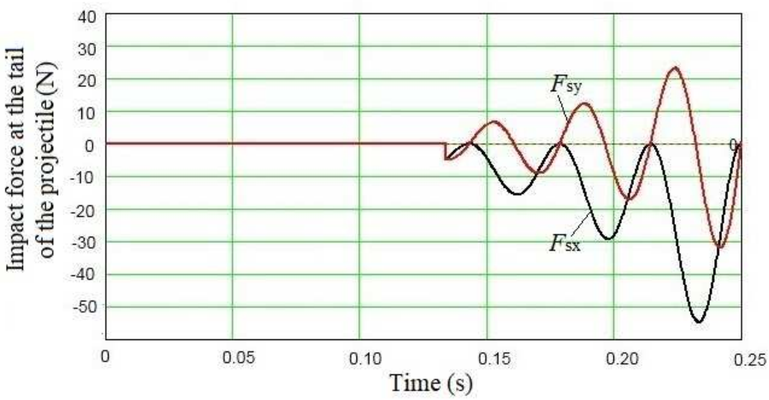

Fig. 9 Impact force at the tail of the projectile vs. time in vertical F_{sy} and horizontal F_{sx} direction

The decrease in the projectile velocity v is examined for the first 0.1 second. The velocity decreases from the muzzle velocity to 112.5 m·s $^{-1}$ and the traveling distance is 16.45 m from the barrel muzzle, see Fig. 10.

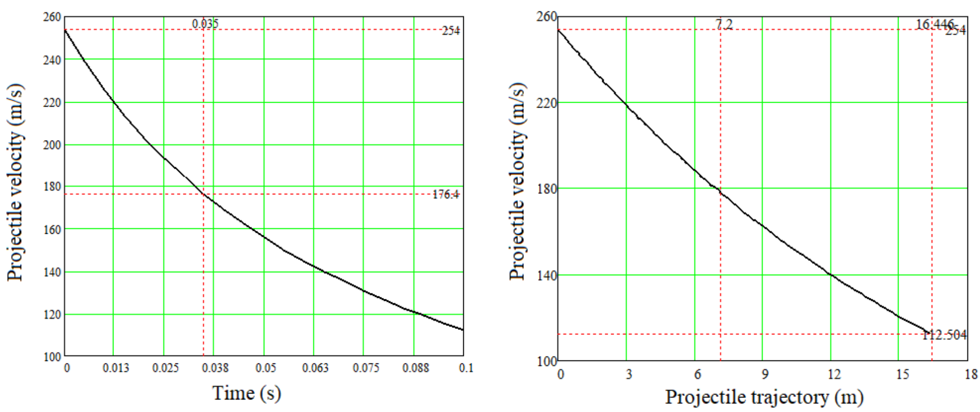

Fig. 10 Time dependence of the projectile velocity and velocity of the projectile vs. its trajectory

4. Verification of Mathematical Model

Computation results of the projectile velocity and the supercavity geometrical parameters are compared with the measured values. Experiments were held in the Weapon Technology Centre of the Le Quy Don Technical University in Hanoi. The schematic of the experimental setup is shown in Fig. 11. Here, the high-speed camera SA1.1. FASTCAM (675 000 frames·s $^{-1}$) was used to record the projectile motion and the supercavity formation.

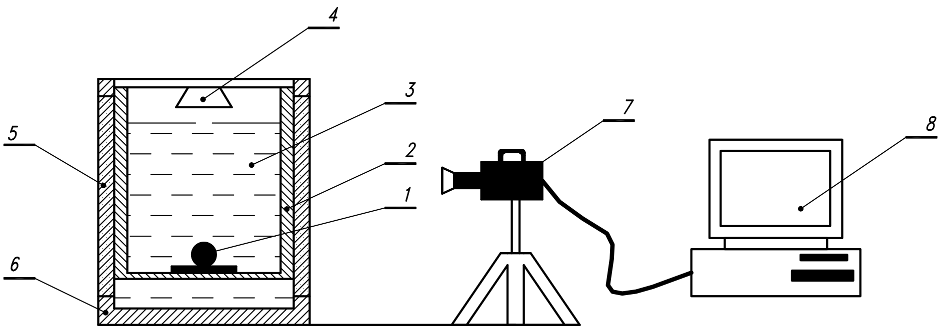

Fig. 11 Schematic of underwater ballistic setup: 1 – ballistic barrel, 2 – gun frame holder, 3 – water basin, 4 – light source, 5 – transparent walls, 6 – water tunnel, 7 – high-speed camera, 8 – computer.

The photograph of the underwater ballistic setup with the ballistic barrel is shown in Fig. 12.

Fig. 12 Photograph of underwater ballistic setup

The process of the supercavity gradual formation can be observed in Fig. 13. The first phase of the cavitation inception is characterized by small vapour bubbles as seen in Fig. 13a. Further, in the second phase, the cavitation is partially formed and the bubbles grow unstably, see Fig. 13b and Fig. 13c. The third phase, when the supercavity is fully developed and encompasses the whole projectile, can be seen in Fig. 13d. Here, we can see that the supercavity shape is close to the elliptical form. Next, the partial cavitation appears again and then entirely disappears due to the drop in the projectile velocity, as can be seen in Fig. 13e and Fig. 13f.

The projectile velocity is measured at a distance of 7.2 m from the muzzle. The calculated (Fig. 10) and experimentally obtained values of the projectile velocity are given in Tab. 1.

a)

b)

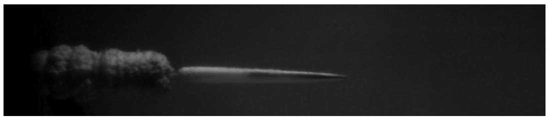

c)

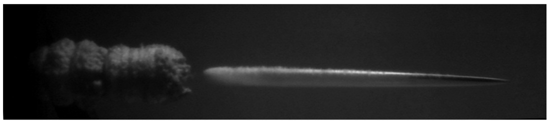

d)

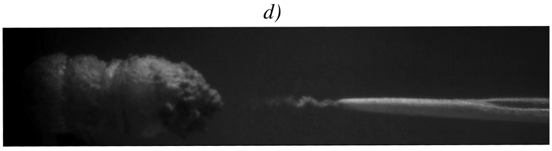

e)

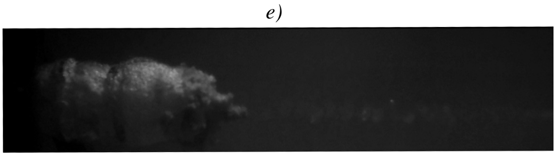

f)

Fig. 13. Supercavity formation recorded by high-speed camera

Tab. 1 Projectile velocity at distance of 7.2 m *from muzzle*

	Experiment	**Model**	**Difference**
Projectile velocity [m·s^{-1}]	177	175	1.1 %

The comparison of theoretically calculated and experimentally obtained dimensions of the fully developed supercavity is shown in Fig. 14.

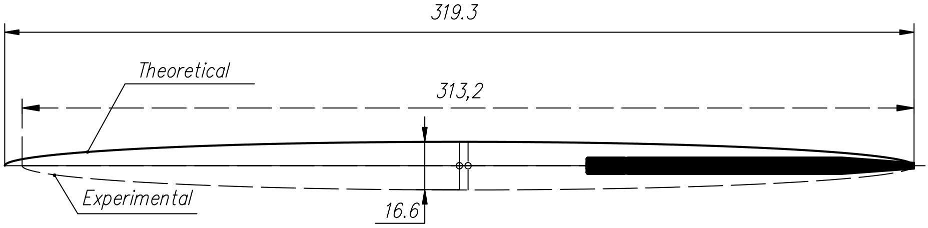

Fig. 14. Comparison of calculated and measured geometry of supercavity in [mm]

Conclusion

In this article, the mathematical model of the underwater projectile motion has been developed. The novel underwater ballistic model has been derived that describes the motion characteristics of the projectile with the nose disk cavitator, which is specially designed for the underwater use. This model also includes the mechanism of water supercavity formation and the influence of the interaction between the projectile and the supercavity during the projectile motion.

The model was validated for the case of 5.7 mm underwater cartridge. There are presented the main ballistic characteristics and the supercavity dimensions for the given underwater projectile. The mathematical model was experimentally verified by measurement of the projectile velocity and the supercavity dimensions by using a high-speed camera. The model provides an excellent agreement with the measured projectile velocity (Tab. 1). In addition, the calculated values of supercavity dimensions also correspond very well with the measured geometry (Fig. 14).

The developed model of underwater ballistics can be used as a powerful tool for designing ammunition for underwater use and understanding the processes of water supercavity formation.

Acknowledgement

The work presented in this paper has been supported by the Weapon Technology Centre and the Faculty of Weapons, Le Quy Don Technical University in Hanoi and by the specific research project of Faculty of the Military Technology SV18-216, University of Defence in Brno.

References

[1] TULIN M.P. *Cavitation, Handbook of Fluid Mech*anics. McGraw-Hill Book, 1961.

[2] FEDORENKO, N.S., KOZENKO, V.F. and KOZENKO, R.N. *Experimental Study of the Inertial Motion of Supercavitating Models*. Berlin: Springer, 2012.

[3] LOGVINOVICH, G.V. *Hydrodynamics of Free-Boundary Flows*. Jerusalem: Program for Scientific Translations, 1972. [Translated from Russian, Gidrodinamika techeniya so svobodnymi granitsami, Kyiv: Naukova dumka, 1969]

[4] VLASENKO, Y.D. Experimental Investigation of Supercavitation Flow Regimes at Subsonic and Transonic Speeds. In *5th Int. Symposium on Cavitation*, Osaka: 2003.

[5] LOYTSYANSKY, L.G. About Change of Body Drag by Filling the Boundary Layer by Liquid with Other Physical Constants (in Russian). *J. Prikladnaya matematika i mechanika*, p. 114-125, 1942.

[6] VASIN A.D. Some Problems of Supersonic Cavitation Flows. In *4th Int. Symposium on Cavitation*, Pasadena: California Institute of Technology, 2001.

[7] SEMENENKO, V.N. Artificial Supercavitation. Physics and Calculation. In *RTO Lecture Series 005, Supercavitating Flows*. RTO/NATO, 2002.

[8] SEMENENKO, V.N. Dynamic Processes of Supercavitation and Computer Simulation. In *RTO Lecture Series 005, Supercavitating Flows*. RTO/NATO, 2002.